International Information and Engineering Technology Association
Advancing the World of Information and Engineering

Mathematical Modelling of Engineering Problems
Vol. 12, No. 11, November, 2025, pp. 3799-3816
Journal homepage: http://iieta.org/journals/mmep

Analysis of Heat Transfer Mechanisms in Multi-Helical Tube and Shell Heat Exchangers Using Computational Fluid Dynamics

Ahmed Abdulmohsen Naji[1], Aseel Kais Rasheed[2], Ayad K. Hassan[3*], Muhammad Asmail Eleiwi[4], Hasan Shakir Majdi[5]

[1] Technical Institute-Suwaira, Middle Technical University, Wasit 52001, Iraq
[2] Research and Technology Center of Environment, Water and Renewable Energy, Scientific Research Commission, Baghdad 10070, Iraq
[3] College of Materials Engineering, University of Technology-Iraq, Baghdad 10066, Iraq
[4] Electromechanical Engineering Department, College of Engineering, University of Samarra, Samarra 34010, Iraq
[5] Department of Chemical Engineering and Petroleum Industries, Al-Mustaqbal University College, Babylon 51001, Iraq

Corresponding Author Email: 130048@uotechnology.edu.iq

https://doi.org/10.18280/mmep.121106

Received: 2 May 2025
Revised: 30 July 2025
Accepted: 8 August 2025
Available online: 30 November 2025

Keywords:
laminar flow heat transfer, boundary layer thickness, Reynolds number effects, thermal efficiency optimization, convective heat transfer

ABSTRACT

The study investigates the heat transfer performance of multi-helical tube-and-shell heat exchangers under low liquid flow rates via computer simulations. It identifies the effects that changing the inlet velocities from 0.2 m/s to 0.6 m/s, and then 1 m/s, had on heat transfer efficiency, boundary layer formation, and temperature distribution. Heat transfer rates increase when the inlet speed is adjusted because the flow rate influences boundary layer thickness and improves fluid mixing. The system at 0.2 m/s exhibited a significant temperature variation because the thick boundary layer and poor fluid mixing produced 31℃ cold water at the outlet. When the system reached 0.6 m/s, the outlet temperature decreased to 24.9℃ because the flow boundary layer had become more compact. Maximum system functionality occurred at 1 m/s velocity because the temperature of the outlet cold water was maintained at 22℃ along with consistent uniform distribution, which demonstrated strong convective heat transfer while minimizing temperature differences between the core fluid and wall. Each simulation was conducted at a different velocity, which produced Reynolds numbers of 275, 824, and 1374—confirming that laminar flow existed throughout the study. This research demonstrates that Computational Fluid Dynamics (CFD) is a valuable tool for modeling heat exchangers operating in laminar flow. A higher inlet velocity of 1 m/s yields the best heat transfer results. This research proposes a new model for optimizing heat exchange in multi-helical heat exchangers, clarifying how characteristics of different flow velocities can contribute to forming a boundary layer. The results hold practical significance for the engineering field, which allows precise design of industrial heat exchangers and ultimately, improved thermal efficiency in energy-demanding industries such as HVAC systems or industrial cooling applications.

1. INTRODUCTION

The helical tube heat exchanger finds rising applications in industrial settings because it combines high thermal performance with compact design and efficient heat transfer abilities. A helically shaped tube arrangement makes up these exchangers because the secondary flow regimes and turbulence boost heat transfer performance. Such heat exchangers experience performance changes through tube geometry and number of turns, flow configurations, and Reynolds number effects. The modeling and optimization of heat exchanger systems through Computational Fluid Dynamics (CFD) requires ANSYS software as a crucial tool for simulations. The review surveys current investigations on helical tube geometry and configuration influence on heat exchanger performance while analyzing outlet temperature and heat transfer together with velocity distribution and pressure drop effects and overall system efficiency [1]. Heat transfer efficiency reaches its maximum level within helical tube heat exchangers because their helical configuration generates secondary flow patterns that increase thermal exchange capabilities. Ferng et al. [2] studied how well helically coiled tube heat exchangers transfer heat using CFD simulations, looking at different Dean numbers and pitch sizes. Higher Dean numbers combined with smaller pitches granted better heat transfer performance because they created increased turbulence and better mixing within the coil structure. Reddy et al. [3] studied the relationship between different tube structures and their influence on heat transfer performance, together with pressure drop evaluations. The model produced by CFD simulation showed better heat exchange after adding more helical turns to the coil, but this caused higher fluid friction, which increased overall pressure drop. For efficient heat exchanger design, the optimal relationship between turn number and pressure drop needs to be reached, according to their findings. Jiang et al. [4] showed that implementing spiral fin-and-tube heat exchanger tubes would boost the performance of shell-and-tube heat exchangers. Using tube fins under optimal flow conditions demonstrated improvements in heat transfer performance and energy efficiency during testing, as reported in the study. Under specific operating conditions, the success of tube design optimization requires detailed CFD simulations to remain constant. Pawar and Sunnapwar [5] delivered an extensive review of helical coil heat exchangers regarding convective heat transfer analysis. Experimental and CFD methods received attention from researchers who studied the behavior of heat transfer in helical coils across different operating conditions. The research looked at two kinds of fluids: regular fluids like water and mixtures of glycerol and water, as well as thicker fluids made from diluted polymer solutions using Sodium Carboxy Methyl Cellulose and Sodium Alginate. Experimentally measured data from a wide parameter space of Reynolds numbers (Re) and Prandtl numbers (Pr), together with coil curvature ratios (a/R), received evaluation through FLUENT solver simulations. The paper brings forward an innovative dimensionless M number to evaluate helical coil hydrodynamics, which includes factors that prior studies overlooked. The analysis of a double helically coiled tube heat exchanger's heat and flow attributes by using Multi-Walled Carbon Nanotube (MWCNT)/water nanofluids was the focus of the study conducted by Kumar and Chandrasekar, which employed CFD. Research results demonstrated that MWCNT/water nanofluids outperformed standard fluids for thermal transfer optimization. According to the study's findings, the helical coil configuration improved heat transfer. Research identified a direct connection between MWCNT nanofluid concentration levels and thermal operation effectiveness since elevated concentration rates produced superior outcomes. The study [6] found that the Re and how curved the coils are affect how liquid flows in the heat exchanger and the pressure drop in the device. Understanding nanofluid-based heat exchangers receives substantial advancement through this research, especially when the aim is to improve thermal efficiency. Sharifi et al. [7] studied how helical wire inserts affect heat and resistance in double-pipe exchangers using CFD. Research results indicated that heat exchange rates rose significantly after installing helical wire inserts because of their flow-induced turbulence, together with mixing activity. Effective heat transfer occurred through secondary flows that resulted from their implementation. Compared to uncoiled tubes, wire inserts demonstrated better heat transfer performance and larger temperature differences in the ANSYS FLUENT models. The study revealed that pressure drops increased due to wire inserts because they elevated the friction factor, although they boosted heat exchange rates. The study conducted a thorough analysis of wire diameter, pitch intervals, and cooling operation parameters. Such research becomes essential for organizations whose heat exchangers must operate with high energy efficiency while dealing with flow resistance limitations. The principal role of heat exchangers is heating enhancement, but minimization of pressure drop remains essential for reducing operating fluid energy needs. A helical tube heat exchanger experiences heightened pressure drops when additional turns are implemented, according to Jayakumar et al. [8]. However, this pressure increase does not exceed the enhanced heat transfer capability. The researchers stressed how designers must handle this pressure trade-off properly since excessive pressure reductions lead to elevated operation costs. The review by Marzouk et al. [9] presented detailed information regarding passive methods that boost thermal performance in helical tube heat exchangers. These devices have gained popularity in thermal systems because of their improved thermal characteristics and compact dimensions. The authors combined multiple heat enhancement strategies by integrating internal inserts and making surface modifications with vortex generator applications. This enhanced thermal performance while keeping pumping power and pressure drop within acceptable levels. The authors explained how various methods affect thermohydraulic performance and stressed that geometric optimization optimizes heat transfer rates. The review showed that combining passive enhancement methods with new materials creates promising research opportunities for sustainable energy systems. The research is a starting point for developing modern heat exchangers that achieve effective performance while conserving power. Sunny et al. [10] explored helical coiled heat exchanger thermal and fluid dynamic procedures through CFD studies on tube-in-tube setups. The heat transfer performance benefited from forming secondary flow patterns, which resulted from curvature effects. Research found that by establishing a connection between Re and coil sizes, it became possible to achieve enhanced thermal performance at acceptable pressure levels using adequate flow rates and small coil diameters. The research confirms that CFD tools enable engineers to design optimal compact heat exchangers that maximize their performance in thermal management systems. Dhumal and Havaldar [11] performed experimental research about maximizing thermal performance of double-tube heat exchangers by deploying twisted and helical tapes as passive enhancement techniques. The researchers established that discharging these tapes generated elevated turbulence intensity, which boosted convective heat transfer performance without causing a pressure drop. The disruption of thermal boundary layers proved more effective in helical tape configurations than regular twisted tape systems because helical tapes produced superior thermal boundary-layer disruption. Heat transfer systems that need greater heat flow together with minimal pumping power now have their efficiency improved by implementing structured inserts, as proven through research findings. Heeraman et al. [12] conducted experimental research on a double-pipe heat exchanger by testing twisted tape inserts with dimple configurations. The study determined which dimple shapes gave the best Nusselt number outcomes with minimized friction factor results because Nusselt numbers directly matched Re changes. Research conducted by Hong et al. [13] investigated a waste heat recovery heat exchanger equipped with spiral corrugated tubes that included multiple twisted tapes. Using perforated twisted tapes in flow systems creates better flow patterns and heat distribution, leading to a higher local Nusselt number and lower friction factor. The system's thermal performance reaches 7.9 percent improvement through the use of perforated twisted tapes. Dhumal and Havaldar [14] showed that tube heat exchangers experienced enhanced thermal effectiveness at the cost of performance decrease due to turbulator-induced secondary swirl flow. When high Re and low twist ratios were combined, it led to more heat transfer that couldn't be reversed, because the friction from the fluid was less significant than the heat movement. The Bejan number approaching one makes heat transfer processes significantly irreversible. Fetuga et al. [15] researched circular tubes with twisted tapes and cylindrical baffles using a mixture of three nanofluids (SiO_2 + ZnO + CaO). This study evaluated the Nusselt number with pressure drop, the thermal performance factor, and pumping power across the flow conditions of laminar flow at Re starting from 500 and ending at 2000, together with nanofluid volume fractions ranging from 0.01% to 0.05%. Experimental findings demonstrated that Nusselt number elevation occurred together with improved thermal performance factor, which makes heat transfer more efficient. Table 1 compares the findings across studies and highlights gaps in the literature that this study addresses.

Table 1. Literature review research gaps

Aspect	Previous Studies	Gaps Addressed
Helical coil heat exchanger performance	Ferng et al. [2] found that higher dean numbers and smaller pitch sizes increase turbulence, thus improving heat transfer. Reddy et al. [3] noted that adding more turns improves heat transfer but raises fluid friction, causing a pressure drop.	Multi-coil configurations for heat exchangers haven't been widely studied.
Re and flow characteristics	Jiang et al. [4] presented that higher Re improves performance in spiral fin-and-tube heat exchangers.	The study addresses the laminar flow regime at lower Re (Re < 2000).
CFD simulations and model validation	Pawar and Sunnapwar [5] demonstrated the importance of CFD simulations for predicting heat transfer efficiency.	Existing studies lack detailed validation of CFD models using recent studies, especially for multi-helical tube heat exchangers.
Fluid flow and heat transfer	Sharifi et al. [7] showed that wire inserts cause flow-induced turbulence and enhance heat transfer, but at the cost of pressure drops.	Previous studies often focused on turbulent flow.
Effect of boundary layer thickness	Marzouk et al. [9] focused on passive methods to optimize heat transfer, but boundary layer dynamics were not the central focus.	The influence of boundary layer thickness in laminar flow has been underexplored, especially under multi-coil geometries.
Helical tube geometry's impact	Kozłowska and Szkodo [16] showed that helical tubes improve heat transfer compared to straight tubes under laminar flow, with better performance at higher Re.	While helical tubes have been studied, multi-coil geometries haven't been fully explored, particularly under laminar flow conditions.

2. METHODOLOGY

2.1 Four helical coils and shell modeling

A three-dimensional flow domain is used in this investigation to estimate input velocity effects in four helical tubes and a shell. The simulation geometry designed by ANSYS CFD 2024 R1 is a modular design with four helical tubes used as a hot fluid domain and an outer shell, which was designed by the same design software, used as a cold fluid domain. The input and outlet points for both cold and hot fluids are designed to flow in opposite directions inside the heat exchanger. After that, the designed geometry was exported to ANSYS CFD 2024 R1 to complete the mesh process and solve the governing CFD simulation equation, and finally, the simulation was run. The four helical tubes, shell geometry dimensions, and physical properties are illustrated in Table 2. Figure 1 demonstrates the modeling of four helically coiled tube heat exchangers used in this CFD analysis.

Table 2. Helically coiled tube and outer shell dimensional parameters

Item	Value
Diameter of Tube Coil	5 mm
Internal Diameter of Outer Coil	25 mm
External Diameter of Outer Coil	30 mm
No. of Coils Turns	10
Coil Overall Length	145 mm
Shell Outer Diameter	110 mm
Shell Overall Length	145 mm
Thermal Conductivity of Copper	401 W/m K
Density of Copper	8960 kg/m^3

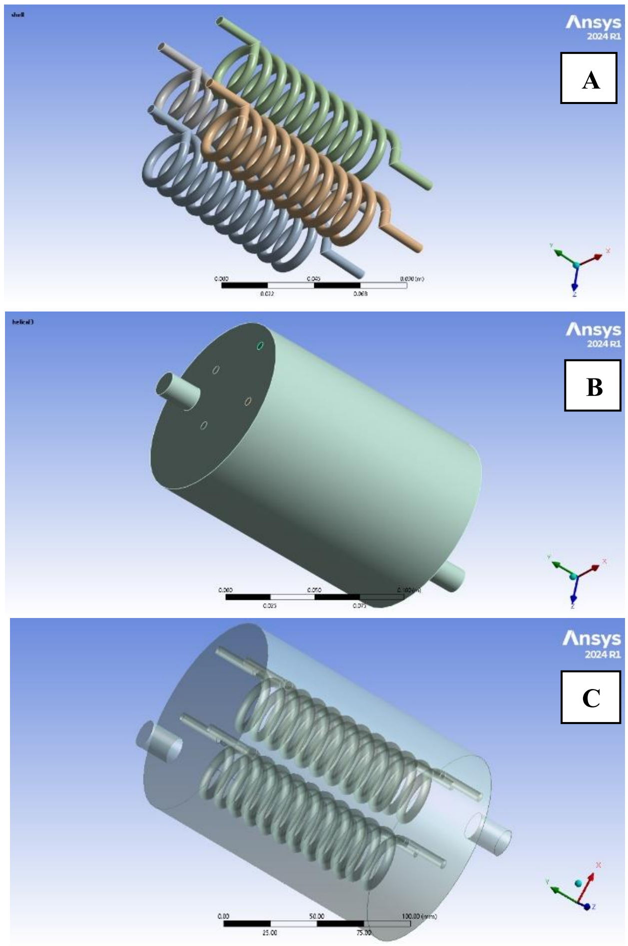

Figure 1. ANSYS modeler geometry design (A) helical coils design, (B) shell design, (C) helical coils and shell assembly

2.2 Re calculations

Re is a critical factor in fluid dynamics because it establishes the flow pattern of fluids in systems. The behavior of fluids and the operational performance of heat exchange processes depend on the Re. The computational process of CFD simulations demands calculating Re for multiple fundamental reasons. The flow condition classification occurs through Re computation because it distinguishes between three types of flow: laminar, transitional, and turbulent. The smooth flow pattern of laminar behavior occurs at Re below 2000, but turbulent flow with its disordered patterns appears when Re exceeds 4000 [17]. The transitional flow regime occurs between 2000 and 4000 Re because the flow maintains an uncertain status between laminar and turbulent conditions. CFD model selection for turbulence simulation depends on determining the Re value. Using laminar flow modeling requires simple models for systems experiencing laminar flow conditions, yet requires advanced models such as k-ε or k-ω modeling in turbulent systems. The precise anticipation of turbulence patterns determines heat transfer outcomes, pressure loss values, and system performance levels. The pressure drop observed in a system depends on the Re as one of its main variables. The knowledge of Re before simulation helps generate better predictions for energy usage and system operational effectiveness [18]. Re evaluation within the helical coil requires understanding the following information update. Outer tube diameter (Do) will be 5 mm (0.005 m), and the Inner tube diameter (Di) will be 4 mm (0.004 m). Inlet hot water temperature will be 77°C, and cold water inside the outer shell inlet temperature will be 10°C. Inlet velocities of 0.2, 0.6, and 1 m/s will be used to compute Re for each case. The Re is calculated using the following formula:

$$Re = \frac{\rho u D_h}{\mu} \tag{1}$$

where, ρ is water density at 77°C, approximately 975 kg/m³, u is the inlet velocity at m/sec, μ is water dynamic viscosity at 77°C, approximately 0.355×10^{-3} kg/m·s, and finally D_h is the tube hydraulic diameter calculated by the following formula:

$$D_h = \frac{D_{0\,tube} - D_{in\,tube}}{2} \tag{2}$$

All inlet flow patterns in the system yield Re under 2000 with initial velocities at 0.2 m/s corresponding to Re = 275. The Re at 0.6 m/s equals 824, corresponding to Laminar flow due to Re < 2000. With a speed of 1 m/s, the Re is established at 1374, which indicates Laminar flow (Re < 2000). The helical coil demonstrates laminar flow because all three inlet velocities measure less than 2000. In straight pipes, switch-ins in the flow usually happen at Re = 2300, where the laminar to turbulence switch takes place. Nevertheless, geometrical curvature and centrifugal effect may move the critical Re of helical or coiled tubes. These cause secondary flows (Dean vortices), and these can, under some circumstances, stabilize the flow and delay transition, or can, instead, introduce instabilities at lower Re, speeding transition. Since the research focuses on inlet rates that lead to Re resembling 1300 to 1400, the system will run in laminar-turbulent. It will not manifest the transition point of curved structures. A small perturbation, like flow pulsations, inlet turbulence, or buoyancy forces driven by temperature, might make the system lose stability and enter transitional flow.

2.3 Boundary conditions and simulation assumptions

The hot water domain utilized different inlet speeds of 0.2 m/s, 0.6 m/s, and 1 m/s at the Four Helical Coils. At the inlet point, hot water entered with a temperature of 77°C. Laminar flow occurs throughout the entire structure of the coils. Every case setup requires an explicit application of external heat fluxes. The Shell Inlet Conditions accept the parameter that determines the Cold-Water Domain's initial movement speed. The analysis uses identical water velocity for hot water, yet reversed. The temperature of cold water entering the system has been established at 10°C. An area of laminar flow exists in the domain where cold water flows. The tube surfaces receiving hot water require a zero-velocity condition, which represents the no-slip boundary. The heat transfer dynamics between hot water and tube wall surfaces depend on the thermal conductivity value of copper at 401 W/m·K that appears in the data table. The outer shell surface (cold water side) also receives the boundary condition of no slip. The imperfect thermal junction between the coils and shell needs special consideration through thermal contact resistance [19]. The Laminar Flow Solver serves both domains (hot water and cold water) because their fluid movement operates under laminar conditions. The simulation operates with steady-state behavior since fluid characteristics and velocities maintain constant rates at every point in time. The mathematical simplifications become possible due to this valid assumption, which applies to systems that maintain fixed flow rate conditions while operating at consistent temperatures. The simulation considers two incompressible fluids that enter as a hot water inlet fluid and cold water in the outer shell. The assumption holds because water density shows minimal variation during typical heat exchanger-operating temperatures. During the simulation, we maintain the belief that fluid density remains consistent. During simulation, all thermophysical water properties, including viscosity, density, and specific heat, remain constant within the simulation domain. Hot and cold water temperature properties are estimated at an average system temperature value, which usually originates from inlet and outlet measurements [20]. The pure convective heat transfer between hot and cold fluids can be calculated using helical coil correlations to evaluate the convective heat transfer coefficient. The fluid displays perfect behavior since we won't estimate any chemical or phase transformation. The model stays simple because the heat exchanger design assumes no boiling or condensation takes place, thus bypassing the requirement for phase-change calculations. Standard correlations help us calculate pressure drops that occur throughout the helical tube system. The Darcy-Weisbach equation, with comparable empirical formulas, serves as the method for determining friction forces and pressure drops in helical coil structures. The performance modeling of the heat exchanger requires this information to forecast both fluid pumping energy needs and system performance accuracy. The heat transfer coefficient inside helical coils remains constant because existing equations for helical fluid flow determine it according to either Dittus-Boelter theory for fast-moving fluids or Sieder-Tate theory for slow-moving ones. The heat exchange between hot and cold water depends significantly on the heat transfer coefficient value. The helical coils show an ideal heat exchange between fluids and coil walls, not including fouling or scaling. The thermal resistance stays fixed between the fluid material and the coil surface, which ensures continuous heat transfer performance regardless of socioeconomic contamination.

The simulation model does not impose a slip boundary condition at the bounds of the helical tube (one that the hot water flows), in addition to the outer shell (one that the cold water flows). This supposition holds both in hot and cold fluid areas. The study does not mention the application of any more sophisticated wall functions (such as increased wall treatment models under turbulent flow), as the analysis is done under laminar flow. The boundary condition of no-slip is used at the tube walls without any treatment of the walls regarding turbulence.

The current study modeled the coils with a constant wall-temperature boundary condition instead of a continuous heat-flux boundary condition. The temperature of the tube-wall was thus held at a constant value of 368.15 K (95℃), which is close to an idealized condition whereby the heating medium, e.g., steam or thermal fluid, is used to provide a uniform wall temperature across the surface of the complete coil. This design allows for the analysis of the convective heat transfer between the wall and the cold fluid within the shell to be done with rigor. In the case of the flow boundaries, the inlet conditions were laid down as that of velocity, whereby the inlets of the shell and tube sides were set as inlet velocity conditions of the fluid, with its cold side inlet having a range of 0.2 to 1.0 m/s, and the fluid was maintained as an inlet temperature condition of 300.15 K (27℃). The pressure outlets on the left and right were characterized as 0 Pa gauge pressure, allowing the fluid to leave freely. No-slip walls were given to all wall surfaces, including the coil and the shell, i.e., the fluid velocity at the wall surface was zero. All these boundary conditions create an ideal heat transfer process model, which is laminar, single phase, steady state, that was sufficiently controlled to obtain equivalent behavior of a multi-helical coil and shell heat exchanger.

2.4 Simulation mesh parameters and testing

The foundation provided by meshes plays a crucial role in obtaining accurate physical phenomenon solutions when using CFD. Simulation accuracy directly correlates to the degree of mesh development accuracy. The physical domain mesh divides its territory into numerous cells, which approximate solutions for fluid motion, heat transfer, and system variables. Precise resolution of velocity, temperature, and pressure gradients depends on a mesh made with proper design. The accuracy of mesh functions is essential because it generates the simulation results. Simulation accuracy in predicting behavioral patterns of real-world systems becomes superior for complex heat exchangers that use proper mesh quality and density standards. One must establish the best possible connection between mesh resolution and computational performance to achieve reliable results. Mesh independence tests serve as standard procedures to identify the most suitable element size because these tests demonstrate minimal result changes while keeping computation costs affordable [21]. Mesh elements require precise definition to enable accurate heat exchanger analysis because they determine both thermal understanding and system optimization capabilities.

Figures 2(A) and (B) illustrate the mesh of the hot water coils and the cold-water outer shell. According to the images in Figure 2, the mesh structure uses unstructured tetrahedral and hexahedral elements with a mesh element size of 1 mm.

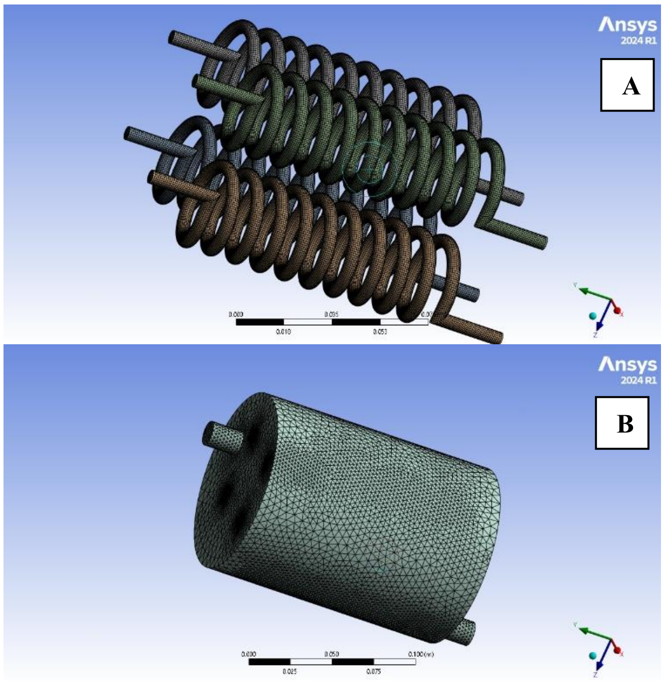

Figure 2. Simulation model mesh (A) four coil design mesh, (B) the complete simulation model design

Table 3. Mesh statistics and methods

Item	Value
Elements size	3 mm
Elements no.	4251195
Nodes no.	1055190
Mesh method	Automatic
Corner nodes	1055190
Solid elements	4251195
Tetrahedrons elements	3987195
Hex elements	264000

The mesh area targets the internal and outer aspects of Figure 2(A) before presenting the four helical coils alone. Figure 2(B) shows the entire outer shell area, while the mesh tracks the coils to see how fluid interacts with the edges, coil surfaces, and nearby regions. The mesh statistics and methods are illustrated in Table 3.

2.5 Independent mesh test

In ANSYS CFD simulations, it's essential to perform mesh independence tests to check how accurate the simulation results are with different mesh sizes. The main goal is to identify the best mesh density that leads to precise results at a cost-effective computational level. To ensure high-quality mesh independence, we need to run several simulations with various mesh sizes, from rough to very detailed, and check for significant changes in the results. When results stabilize during mesh refinement, mesh independence is indicated because it demonstrates minimal changes. The mesh independence test was simulated with 10 different element sizes, ranging between 1 mm and 10 mm. The element size is the main component determining mesh resolution in this testing process. The analysis produces more mesh elements for small-sized elements and fewer elements when elements are bigger [22]. The test analysis allowed observation of the outlet temperature of the cold water as its primary measurement point. Table 4 below demonstrates the test results graphically represented in Figure 3.

Table 4. Independent mesh test results

Element Size (mm)	Nodes No.	Elements No.	Corner Nodes	Solid Elements	Cold Outlet Temp. (°C)
1	13753338	5951854	13753338	5951854	23.96
2	1091470	4437548	1091470	4437548	22.51
3	1055190	4251195	1055190	4251195	22.85
4	1048686	4219461	1048686	4219461	22.72
5	1046789	4210406	1046789	4210406	21.80
6	1046604	4209543	1046604	4209543	21.04
7	1046429	4209048	1046429	4209048	20.87
8	1046308	4208453	1046308	4208453	20.72
9	1046353	4208419	1046353	4208419	20.52
10	1046624	4210122	1046624	4210122	20.21

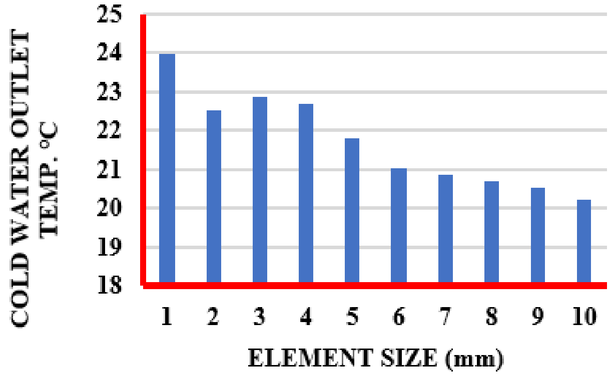

Figure 3. Mesh independent test results graphical chart

Table 4, together with Figure 3, demonstrates that the cold water outlet temperature decreases steadily with increased element diameter (from 1 mm to 10 mm). By increasing the element size from 1 mm to 10 mm, the cold water outlet temperature decreases from 24.5 to about 20°C. Increased accuracy in outcome measurement occurs through a substantial temperature variation at the cold water outlet, which results from changing the element size from 1 mm to slightly coarse (2 mm). Beyond this stage, the element increases, causing the temperature to become more stable and produce less fluctuation. The slight difference between 3 mm and 10 mm element size implies that the simulation endpoint has started to converge. Further mesh refinement will yield minimal changes in the results since the mesh has developed approximate independence.

The accuracy level will remain satisfactory when using 3 mm or 4 mm size elements; however, the calculations will execute faster compared to 1 mm or 2 mm elements. These element sizes manage to find an appropriate equilibrium between computational execution speed and solution precision through their reduced heat flow pattern resolution compared to 1 mm mesh elements. Element sizes of 3 mm or 4 mm offer suitable options for receiving quick results alongside reasonable accuracy in preliminary design studies when high precision is not critical or across model regions where accuracy requirements are lower. The mesh product explains information with reduced detail in flow property change zones (boundary layers and turbulent regions) if element sizes rise above 4 mm. The larger elements in your simulation model reduce accuracy whenever flow separation, vortex shedding, or thermal gradients become significant. These simulations achieve high computational speeds but cause such accuracy to decrease substantially, affecting heat exchanger performance prediction [23].

3. SIMULATION GOVERNORS' EQUATIONS

Computation for different Re and ANSYS FLUENT numerical simulations showed a laminar flow. The following equations were utilized to model and compute the heat transfer between hot and cold water, velocity dispersion, and pressure drop. When hot water flows out of a vessel and into a coil of cold water, the amount of heat lost is determined by:

$$Q = \dot{m}C_p(T_{out} - T_{in}) \tag{3}$$

Except for the heat transfer rate, all other known values are. The total heat transfer coefficient, U_o as, was computed using the heat transfer rate obtained from the previous equation:

$$U_o = \frac{Q}{A_0\, \Delta T_0} \tag{4}$$

The average temperature difference between the fluid in the vessel and the mean bulk temperature of the fluid in the coil (average of the intake and outlet temperatures) and A_0, the outer surface area of the coil, is denoted as ΔT_0. The following equation may be used to get the internal heat transfer coefficient h_i:

$$h_i = \frac{Q}{A_i\, \Delta T_i} \tag{5}$$

T_i is the average temperature differential between the average wall temperature and the average bulk temperature of the fluid in the coil; A_i is the coil's internal surface area, and m is the average temperature taken at various positions on the coil's surface. The coil's inner Nusselt number is then determined using:

$$N_u = \frac{h_i D_i}{K} \tag{6}$$

To determine the coil's outside heat transfer coefficient, one uses:

$$h_o = \frac{Q}{A_o\, \Delta T_o} \tag{7}$$

The difference between shell and coil wall temperatures at their average value is known as T_o. The text implements a data analysis experimental method following an approach similar to Pawar and Sunnapwar [5] through equivalent experimental conditions. In this study, water is considered an incompressible, steady-state, homogenous, Newtonian fluid, with very little influence from viscous heating. The Navier-

Stokes equations, implemented in the ANSYS Fluent package, have been used to simulate the flow. Equations in Cartesian coordinates (x, y, z) for a single-phase homogeneous flow are as follows:

A formula for continuity:

$$\rho\left(\frac{\partial u}{\partial x}+\frac{\partial v}{\partial y}+\frac{\partial w}{\partial z}\right)=0 \tag{8}$$

Navier–Stokes equations (momentum equations):

$$\rho\left(u\frac{\partial u}{\partial x}+v\frac{\partial u}{\partial y}+w\frac{\partial u}{\partial z}\right)=\mu\left(\frac{\partial^2 u}{\partial x^2}+\frac{\partial^2 u}{\partial y^2}+\frac{\partial^2 u}{\partial z^2}\right)-\frac{\partial p}{\partial x} \tag{9}$$

$$\rho\left(u\frac{\partial v}{\partial x}+v\frac{\partial v}{\partial y}+w\frac{\partial v}{\partial z}\right)=\mu\left(\frac{\partial^2 v}{\partial x^2}+\frac{\partial^2 v}{\partial y^2}+\frac{\partial^2 v}{\partial z^2}\right)-\frac{\partial p}{\partial y} \tag{10}$$

$$\rho\left(u\frac{\partial w}{\partial x}+v\frac{\partial w}{\partial y}+w\frac{\partial w}{\partial z}\right)=\mu\left(\frac{\partial^2 w}{\partial x^2}+\frac{\partial^2 w}{\partial y^2}+\frac{\partial^2 w}{\partial z^2}\right)-\frac{\partial p}{\partial z} \tag{11}$$

Energy equation:

$$\rho\left(u\frac{\partial T}{\partial x}+v\frac{\partial T}{\partial y}+w\frac{\partial T}{\partial z}\right)=\frac{\kappa}{C_p}\left(\frac{\partial^2 T}{\partial x^2}+\frac{\partial^2 T}{\partial y^2}+\frac{\partial^2 T}{\partial z^2}\right) \tag{12}$$

where, p, T, u, v, and w represent the pressure, temperature, and velocities in the x, y, and z directions, respectively.

4. RESULTS AND DISCUSSIONS

4.1 Velocity profile effects

Flow in a helical cone coil heat exchanger is significantly disrupted all the way along its length due to centrifugal force generated by the coil's curvature. Before the area was fully established, this flow disturbance became dominant, causing irregular flow and challenges in forecasting. Therefore, the authors had to find a fully formed region to analyze the thermal characteristics of helical cone coil heat exchangers. The heat exchanger's coil contours of velocity flow profiles over the hot water outlet tube cross section are shown in Figures 4(A), (B), and (C) at three different inlet velocities.

We need to understand laminar flow basics before examining its velocity profiles because laminar flow produces organized fluid motion, which maintains separate layers of water throughout its path. At lower speed levels, laminar flow occurs, which results in thermal boundary layers creating themselves along the tube walls. The established boundary layer creates thermal resistance, reducing the heat transfer between the hot tub and external cold water. The fluid structure in laminar flow creates two distinct motions between the bulk flow and fluid neighboring the tube wall.

Heat exchange in laminar flow exists mainly through conduction inside the thermal boundary layer rather than the more inefficient convection. In Figure 4(A), a smooth parabolic shape is visible in the velocity profile, which reaches 0.2 m/s. Among the three profiles, this velocity represents the slowest condition, as fluid motion reaches its highest speed at the tube's central area, as compared to the fluid adjacent to the walls. The tube walls receive thick thermal boundary layers because the inlet velocity remains at a low level. The dense thermal boundary layer opposes efficient heat transfer from hot water to the cool water located in the shell at this slow water velocity. Most heat transfer occurs through conductive processes in the boundary layer, but such conductive transfer proves much less efficient than convective heat extraction [24].

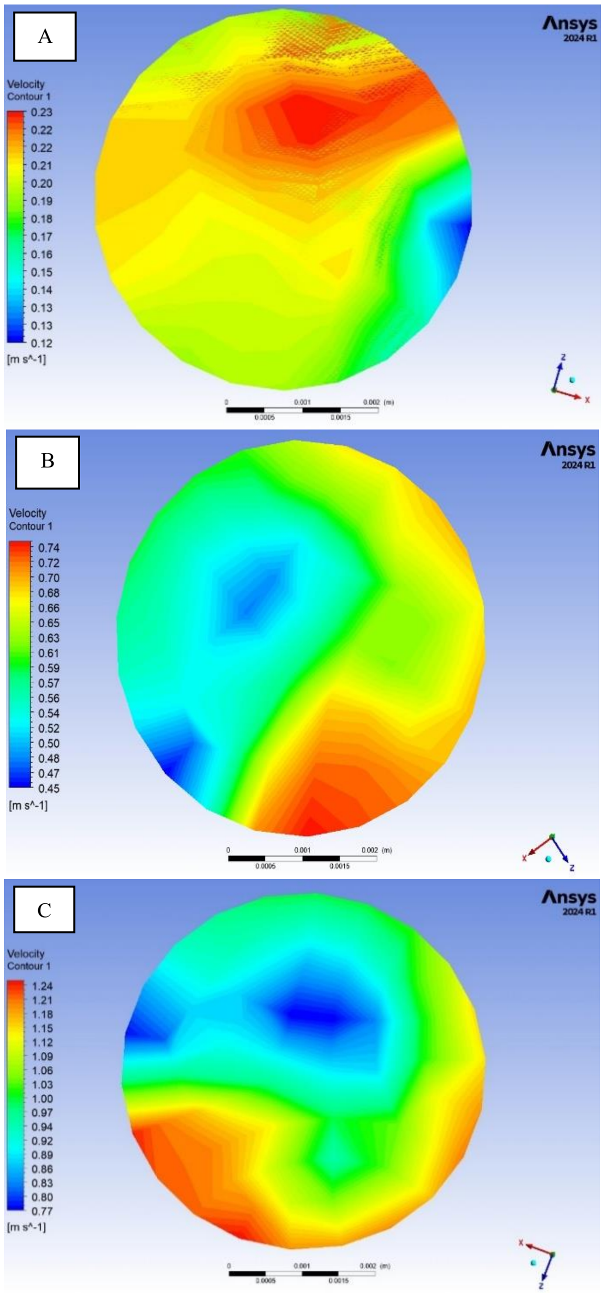

Figure 4. Hot water coil velocity outlet profile (A) 0.2 m/s inlet velocity, (B) 0.6 m/s inlet velocity, and (C) 1 m/s inlet velocity

Between the tube walls, the flow maintains zero movement because this leads to weak convective heat transfer processes, which slow down total thermal exchange. The thermal energy from hot water does not dissipate effectively from tube surfaces because the tube wall fluid moves at a slower pace, thereby creating major temperature variations between the wall and flow area. The velocity profile develops a steeper slope when increasing the velocity to 0.6 m/s in Figure 4(B). A greater velocity exists within this system as the slope between the tube center and wall rises. At this elevated flow speed of 0.6 m/s, the thermal boundary layer grows thinner as a result of the increased velocity when compared to the 0.2 m/s flow. A velocity gradient exists in the system, which demonstrates faster flow motion at the tube center when compared to the wall areas while maintaining laminar flow characteristics. Rising flow speed leads to reduced thickness in the thermal boundary layer. The heat transfer efficiency from hot water to cold water surpasses that of 0.2 m/s because of the implementation of a lower boundary layer resistance. The raised velocity provides heat transfer efficiency that exceeds the values obtained during a velocity of 0.2 m/s. Despite these small advantages, the heat transfer remains limited in laminar flow since it does not produce enough turbulent mixing to achieve maximum convection heat transfer. The velocity profile in Figure 4(C) becomes exceptionally steep at 1 m/s while producing an increased distinction in velocity between the tube's center and walls. An established laminar flow exists, although the velocity gradient becomes more visible. As the boundary layer becomes thinner, the central velocity reaches much higher values than either of the other boundary conditions [25]. The acceleration in velocity does not affect the laminar characteristics of the flow regime. The velocity variation between the central flow region and the external areas of the flow process becomes progressively greater. The velocity's increased speed produces an even more slender thermal boundary layer, which optimizes heat transfer from hot fluid to the surrounding cold fluid. Heat transfer gets better with this improvement, although the flow continues to stay laminar. The decreased thickness of the boundary layer enhances heat conduction performance better than lower flow rates. The increased velocity of flow does not overcome the limiting effects that laminar flow has on heat transfer performance. The fluid velocity next to the wall is exceptionally low, which leads to temperature differences forming between the wall material and the fluid flow region distances. The heat transfer process depends heavily on the geometrical characteristics of the helical tube coil. The coil shape produces secondary flow in laminar streams, generating centrifugal forces that might somewhat destabilize thermal boundary layers. The geometrical properties of the helical tube coil help decrease the boundary layer thickness near walls, thus boosting heat transfer above a plain tube's performance. At turbulent flow conditions, the geometric structure has its most significant influence.

Helical coil creates secondary flow motion during laminar conditions where the resulting turbulence falls below the levels observed in turbulent flow, so its heat transfer contribution remains minimal [26]. Fluid dynamics and heat transfer expertise depend on recognizing the fluid velocity-related effects on thermal exchange to optimize heat exchangers and similar systems. Research and engineering professionals can use comparative velocity measurements to find essential understandings regarding how flow features control heat exchange efficiency. Compiling data in Table 5 enables simultaneous review of multiple analytical scenarios. Design and operational assessments become more feasible through this method because it depicts distinct patterns as well as design deficits for improvement. Table 5 presents data about the helical tube coil system, where three velocities (0.2 m/s, 0.6 m/s, and 1 m/s) demonstrate their impact on flow characteristics and boundary layer thickness, and heat transfer effectiveness.

Table 5. Velocity profile results comparison

Flow Velocity	Low (0.2 m/s)	Moderate (0.6 m/s)	High (1 m/s)
Velocity profile characteristics	Smooth, parabolic with lower velocity near the walls	Steeper velocity gradient, faster near the center	Steepest velocity gradient, significantly faster in the center
Boundary layer thickness	Thick thermal boundary layer	Thinner thermal boundary layer	Thinnest thermal boundary layer
Heat transfer efficiency	Lowest heat transfer efficiency	Moderate heat transfer efficiency	Improved heat transfer efficiency, but still limited
Convection vs. conduction	Dominated by conduction due to laminar flow	Still conduction-dominated but better than 0.2 m/s	Conduction still dominates, but a thinner boundary layer improves heat transfer
Effect of coiled geometry	Limited impact in laminar flow	Some effect of coiled geometry, but not significant in laminar flow	Slight improvement due to coiled geometry, but not as effective as in turbulent flow

4.2 Hot coil outlet temperature profile analyses

During laminar flow, the fluid displays smooth movement because fluid layers transfer parallel to adjacent layers. The main heat transfer mechanism in laminar flow consists of fluid conduction and heat transfer through the wall boundary layer adjacent to the tube structure. Laminar flow creates a wide temperature contrast between fluid that contacts the wall and fluid in the center because the wall cools quickly while the core remains heated. In cases of laminar flow, the helical tube coil creates secondary flow that minimally disrupts the fluid movement, yet the effect remains weaker than it would in turbulent flow conditions. Figures 5(A), (B), and (C) illustrate the helical tube outlet temperature profile for the three testing speeds. In Figure 5(A), the temperature gradient is very steep and runs through the entire tube cross-section when the flow velocity remains at 0.2 m/s. Positioned at the center of the pipe flow, the hottest temperature exists, while the surrounding fluid near the walls has become cooler because it has exchanged heat with the surrounding fluid shell. In this situation, conduction leads heat transfer operations while creating a wide thermal boundary layer that encircles the tube. The thick boundary layer hinders efficient heat exchange by creating insulation between hot and cold water substances. The temperature difference between hot water near the tube wall and the center of the coil is substantial because the wall temperature remains significantly cooler. The section directly adjacent to the cold fluid contacts hot water becomes the coldest point inside the tube wall. The low speed of flow results in diminished heat transfer capabilities because the tube wall fluid stays segregated from the flow center thermal energy. The laminar flow compounds this problem since it fails to adequately mix fluid, while the heat transfer mainly depends on conduction within the thin wall region [27].

In Figure 5(B), a velocity change to 0.6 m/s diminished the temperature difference across the cross-section. By increasing the velocity, the thermal boundary layer becomes thinner, which results in improved heat transfer between the hot fluid and the cold fluid adjacent to the shell. At 0.6 m/s flow speed, the fluid's central temperature stays warmer than before, yet the heat gradient between the core and the edges of the circulating fluid has decreased substantially in comparison to when the velocity was set at 0.2 m/s. The temperature distribution reveals reduced sharpness of the hot to cold fluid transition compared to 0.2 m/s due to the modified profile at 0.6 m/s. Near the tube wall temperature elevates while the outer areas maintain a cooler condition. An efficient heat transfer occurs because the thin thermal boundary layer enhances the rate at which heat moves from the hot water to the surrounding cold fluid. Because the fluid stays within laminar boundaries, the heat transfer remains compromised while conduction continues to be the primary heat transfer method. During the velocity level up 1 m/s in Figure 5(C), the heating system generates temperature uniformity throughout the cross-section better than previous velocity measurements. Heat loss from the central section throughout the tube length reduces because the central region of the flow remains cooler near the walls. Such velocities thin the thermal boundary layer, thus enabling better heat transfer efficiency. The fluid outlet's middle region dissipates heat quickly, creating an even temperature distribution throughout the cross-section. Compared to previous speeds, the temperature distribution throughout the flow is more uniform because the center maintains elevated temperatures at this velocity level. Better heat transfer performance appears in this visualization because the temperature difference is reduced between the boundary fluid and core fluid. The heat transfer efficiency improves because of the thinner boundary layer at increased velocity, yet the flow maintains laminar behavior. A better temperature spread exists, but the heat transfer primarily functions through conduction; therefore, performance achieves only moderate levels than turbulent operation. The authors note that temperature profiles show different patterns when entering at various velocities. The broader thermal boundary layer at lower velocities restricts the heat that escapes from the tube through its surface into the surrounding water [23]. Also, the boundary layer becomes thinner when velocities rise, yet this effect's heat transfer enhancement remains less dramatic than turbulent flow. Laminarity prevails throughout the flow process, thereby maintaining limited movement between different fluid sections. Due to higher temperature, the core fluid remains separate from the surrounding fluid near the tube walls. A significant temperature variation persists throughout the tube cross-section since the fluids fail to mix. The helical tube shape produces secondary flow patterns that contribute marginally to interferences in the boundary layer formation. These secondary flows show greater effects on heat transfer when the flow condition is turbulent because they increase mixing and improve transfer. The effects of these devices remain marginal under laminar flow conditions.

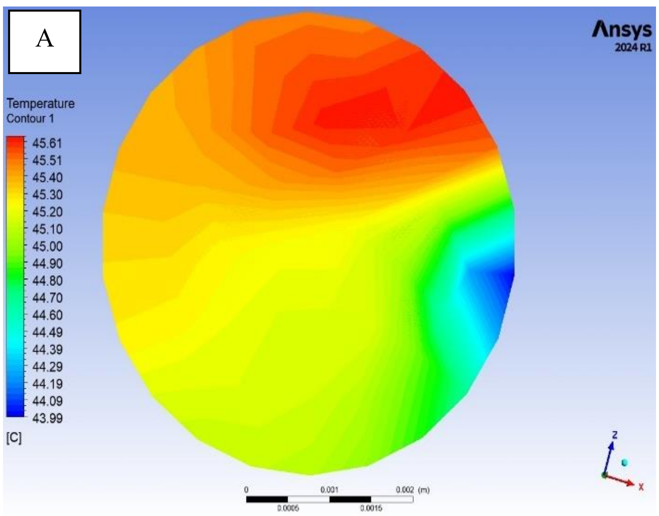

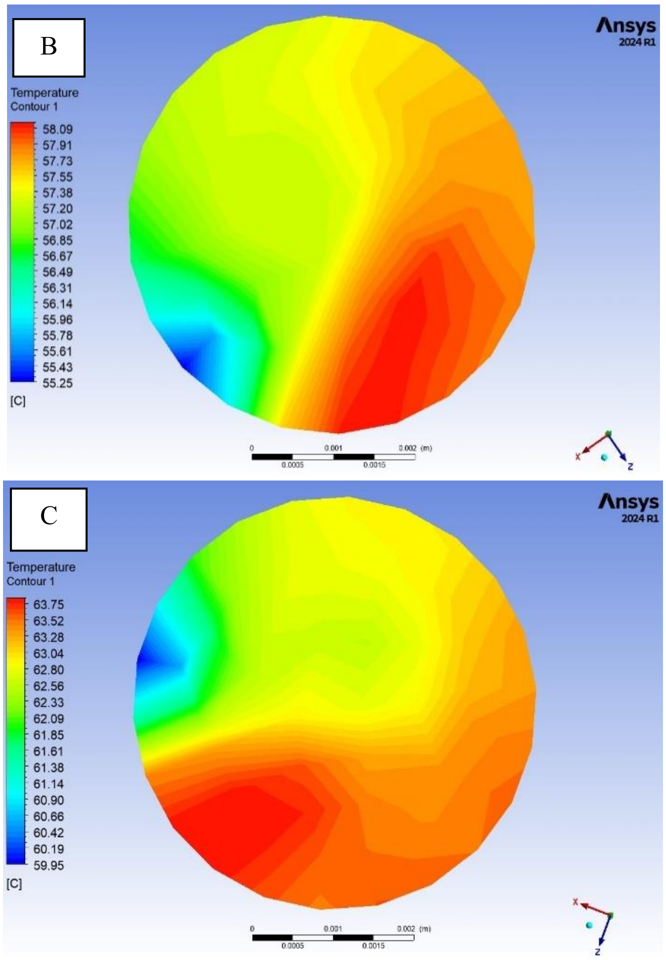

Figure 5. Helical coil tube outlet temperature profile (A) at 0.2 m/s inlet speed, (B) at 0.6 m/s inlet speed, and (C) at 1 m/s inlet speed

According to Figure 5(A), the evaluated temperature data spans between 43.99°C and 45.64°C. The temperatures throughout the central cross-section of the tube probably approach the maximum values of this range, while wall-contacted fluid cools towards the minimum temperature measures. The core fluid temperature shows 45.64°C because the flow has experienced limited heat loss. The hottest part of the profile resides in this segment. At the tube walls, the temperature reaches 44.17°C, which is much lower than the temperature elsewhere. The temperature of the tube wall-cooled fluid decreases because heat transfers between these layers to the surrounding cold fluid. The thermal boundary layer thickness is accomplished at this speed level, which produces an extensive temperature gradient between the internal core region and the external peripheral area. The temperature in Figure 5(B) ranges from 44.17°C to 45.64°C. The dimensionless temperature gradient between the tube core and wall experiences reduced steepness compared to the 0.2 m/s flow condition. The heated fluid near the core maintains temperature levels at 45.64°C, which is slightly cooler than at 0.2 m/s because of enhanced heat transfer. The temperature near the tube walls has become slightly warmer since rising to 44.54°C as compared to the 0.2 m/s flow condition. A better distribution of temperature appears because the boundary layer has become thinner. Higher velocities create thinner thermal boundary layers, which improves the exchange rate between the hot fluid and the surrounding fluid temperature. The temperature spread throughout the system achieves a better balance at higher velocities compared to reduced velocities. The temperature values in Figure 5(C) extend from 59.95°C to 63.83°C. The hot water temperature across the center of the flow remains high because the boundary layer is slimmer compared to other conditions, but the temperature range from 59.95°C to 63.83°C is the highest among all three scenarios. Hot temperatures between 63.83°C and 59.95°C affect the core area of the fluid flow. Better heat transfer emerges from the reduced temperature separation between core and wall when examining 0.2 m/s against the other flow rate. The tube walls have exposed fluid at a temperature of 60.81°C because of enhanced heat transfer compared to lower velocity scenarios. The improved thermal efficiency is notable at increased velocity since heat transfer from the tube reaches the surrounding cold fluid more efficiently. A remarkable trade-off occurs at this flow velocity because the boundary layer has narrowed to improve heat transfer, but the flow remains laminar. The temperature difference between water layers is minimal, while hot water dissipates heat to cold water at a greater rate than the 0.2 m/s condition. Table 6 below summarizes the temperature variation according to the velocity.

Table 6. Temperature ranges at each velocity comparison

Velocity (m/s)	1 m/s	0.6 m/s	0.2 m/s
Temperature range (°C)	59.95°C to 63.83°C	44.17°C to 45.64°C	43.99°C to 45.64°C
Central region temp. (°C)	63.83°C	45.64°C	45.64°C
Wall region temp. (°C)	60.81°C	44.54°C	44.17°C
Boundary layer thickness	Thinnest	Thinner than 0.2 m/s	Thick
Heat transfer efficiency	Highest	Moderate	Lowest

4.3 Hot coil outer wall temperature profile analyses

The fluid layers in laminar flow avoid mixture among all layers. A temperature gradient extends from the central region toward the tube walls because the tube surface transfers heat toward the surrounding fluid. Fluid transport along the tube increases thermal boundary layers, establishing heat transfer insulation that decreases transfer speed. When the fluid speed rises, the boundary layer reduces in width, leading to more efficient heat transfer due to enhanced thermal gradient. Figures 6(A), (B), and (C) demonstrate the heat profile of the helical coil tube at the selected three velocities.

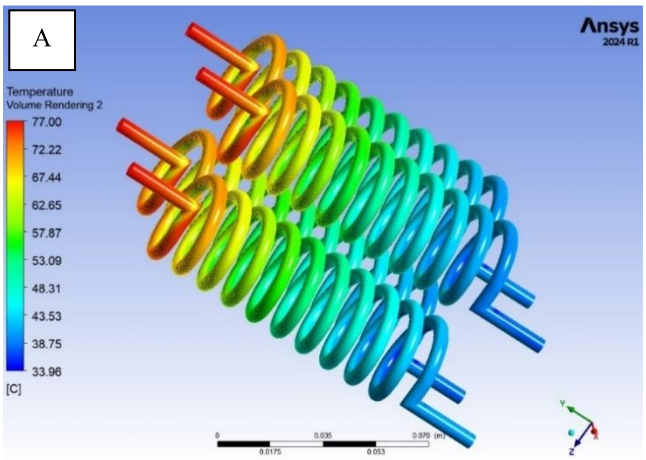

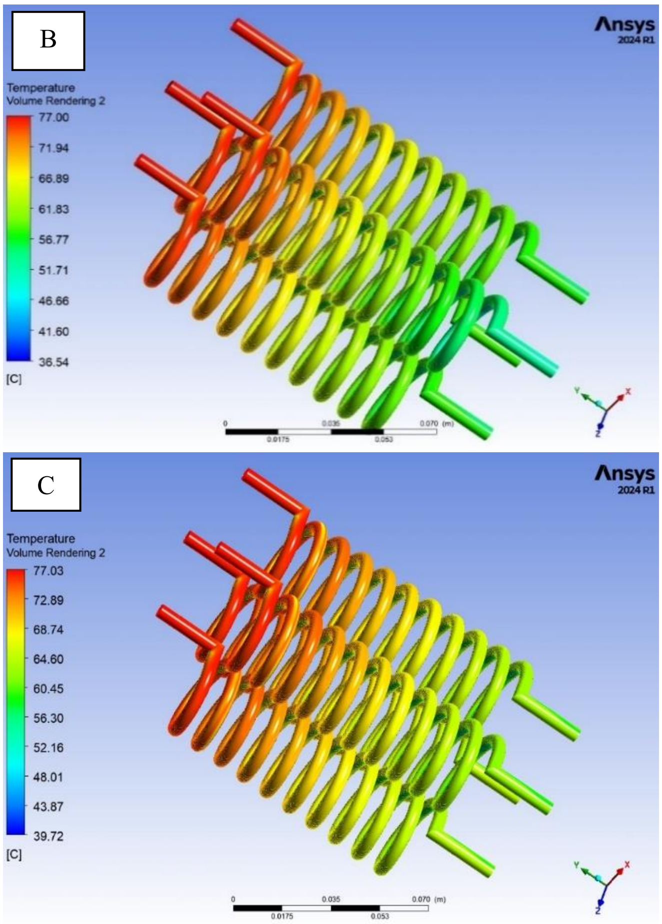

Figure 6. Helical coil tube outer wall temperature profile (A) at 0.2 m/s inlet speed, (B) at 0.6 m/s inlet speed, and (C) at 1 m/s inlet speed

In Figure 6(A), at 0.2 m/s, the outer wall of the hot water tube shows temperature variation between 39.72°C and 77.03°C. Near the inlet of the coil exists the highest temperature range because hot water enters at a higher temperature. A proximity to the walls creates lower temperatures around 39.72°C because heat escapes to the cool ambient fluid. Near the outer part of the coil, the temperatures fall mainly in the lower range because the thermal boundary layer extends generously, resulting in poor heat exchange efficiency. Insufficient heat transfer occurs at low velocities because of an extended thermal boundary layer. The temperature readings of the tube's exterior surface stay cool due to poor thermal conductivity between the hot and cold water. Heat escapes rapidly from the tube wall's outer surface, though the flow speed remains minimal, so convective heat transfer toward the shell water remains limited. The temperature variation measured along the hot water tube outer wall ranges from 36.54°C to 71.94°C when operating at 0.6 m/s in Figure 6(B). The velocity rise has increased the outer wall temperature of the tube to 41.60°C, exceeding the temperature recorded for 0.2 m/s velocity. An improved heat transfer efficiency occurs when the thermal boundary layer becomes thinner. The central fluid region remains hotter throughout, but the outer wall temperature drops gradually because effective heat transfer from the fluid contacts the surrounding cold water. The hot water tube exterior wall temperature spans from 39.72°C to 77.03°C when operating at 1 m/s, as illustrated in Figure 6(C). The highest velocity increases the outer wall temperature to 43.87°C at this velocity since more heat moves from the hot water tube to the surrounding shell liquid. The hot fluid core temperature stays high at 72.89℃, while the outer wall temperature presents uniform distribution across the coil length. The outer wall temperature exceeds earlier readings at the 0.6 m/s and 0.2 m/s velocity settings, yet remains beneath the values of the central region temperature. The fluid velocity's elevated levels generate a reduced thermal boundary layer, making heat transfer more efficient. Improved heat transfer occurs between the hot and cold fluids because of the increased effectiveness of heat distribution. The outer wall temperature shows better performance than earlier velocities did. The continued laminar flow restricts the heat transfer efficiency because it fails to reach the maximal results achieved by turbulent flow regimes. Table 7 presents data about temperature changes and system heat transfer performance at the different inlet flow speeds ranging from 0.2 m/s to 0.6 m/s and 1 m/s. This table provides quick insights into flow velocity effects on heat transfer in laminar flow situations through helical tubes [28].

Table 7. Outer wall temperature and heat transfer efficiency in a laminar flow helical tube coil at different inlet velocities comparison

Velocity (m/s)	1 m/s	0.6 m/s	0.2 m/s
Temperature range (℃)	39.72℃ to 77.03℃	36.54℃ to 71.94℃	39.72℃ to 77.03℃
Outer wall temperature (℃)	43.87℃	41.60℃	39.72℃
Thermal boundary layer	Thinnest	Thinner	Thick
Heat transfer efficiency	Highest	Moderate	Lowest

The entrance region can be considered as an important area of research in helical pipes because it is at this area that the first steps of the thermal and hydrodynamic boundary layer development occur. By gradually reducing the entrance length in increasing succession, the propagation of such layers towards the tube wall is enhanced, increasing the effective surface area of convective heat transfer through convection. At low Re found in low-velocity regimes, the boundary layer is relatively thick and slow to grow, lengthening the transition zone and decreasing the convective heat-transfer coefficient. Besides, the opposite is valid at greater velocities, wherein boundary-layer thinning enhances the transition and produces steeper velocity fluctuations at the boundary, consequently increasing the wall shear stress and the interfacial heat-transfer coefficient. At the same time, the increased field of velocities also performs the simultaneous job of reducing the thermal layer of the boundary adjacent to the wall and increasing the temperature difference, as it is closer to the wall and further away from the wall. The recurved geometry of helical tubes induces centrifugal forces that are not present in straight pipes and cause the Dean vortices. In this case, the fluid near the center flows fast, due to which vortices are formed. The produced centrifugal force gives the fluid inertia and drives it outward to generate two counter-rotating vortices within one pipe cross-section. Due to the thinner thermal boundary layers that come along with the elevated axial velocity, the reinforced Dean vortices produced by the elevated centrifugal force and the enhanced core-wall fluid mixing associated with high axial velocity, the thermal resistance at the wall-fluid interface is weaker; the heat-transfer performance of a helical tube with high axial velocity is better. Along with these makings, the Nusselt number also increases, yielding more heat efficiency. The trend, therefore, means that the cold-end temperature would have a significant rise when the inlet velocity is reduced to 0.2 m/s, when compared to the temperature with an inlet velocity of 1 m/s, at the same outlet velocity of 0.2 m/s; this variation would reflect greater absorption of heat by the hot fluid. The finding is associated with a rise in the convective heat-transfer coefficient related to secondary flows enhanced by the helical arrangement. Though the flow is laminar ($Re < 2000$), curvature-aroused Dean effects play the role of the acting entities as the sources of turbulence even in the laminar range of flows.

4.4 Outer shell inlet temperature profile analyses

The temperature patterns of a heat exchanger shell filled with cold water can be observed through Figures 7(A), (B), and (C), while showing different inlet temperature distributions with velocity conditions from 0.2 m/s to 0.6 m/s and 1 m/s. Research simulations based on ANSYS CFD software-generated profiles will be used to determine the thermal effects that water experiences while flowing inside the shell. The examination in this research investigates the thermal gradient that emerges because the shell wall transfers heat to the flowing cold fluid in laminar flow conditions. The temperature distribution in Figure 7(A) reveals heat accumulation at the outer boundary (shell wall) areas before declining toward the heat exchanger core. The laminar flow nature leads to this particular temperature distribution because the wall boundary layer becomes thicker while heat transfers mainly through conduction between the surface and fluid due to limited mixing. The shell wall's proximity to the fluid generates a thick heat resistance layer because the fluid near the wall moves at a slower speed during laminar flow motion. During laminar flow, heat transfer occurs mostly by conduction since fluid particles mix inefficiently, so convective heat transfer becomes less efficient. A velocity of 0.2 m/s at the inlet creates slow-flowing water, so enough time exists for wall-situated water to absorb heat. The material moves without mixing due to laminar flow, which leads to poor efficiency of heat transfer from the shell wall to its central area.

The distance from the center is the determining factor behind cooling temperatures in the contained area. The lack of mixing, together with poor convective heat transfer, lowers the heat exchanger's efficiency when operating in laminar flow. Water remains inside the shell for an extended period, but inadequate wall-to-center heat transfer decreases the total heat exchange efficiency. The central part of the fluid maintains a cool temperature, indicating inadequate fluid heating [29]. The shell temperature distribution shows improved uniformity under this velocity condition compared to 0.2 m/s, as shown in Figure 7(B). Heat transfers most efficiently from the shell perimeter, but the core area stays chilly. At this velocity, the laminar flow occurs with slightly less constraint than at 0.2 m/s.

Increased water movement at 0.6 m/s maintains laminar flow but reduces water exposure time to heating surfaces. Improved mixing performance happens because of faster velocity in laminar flow conditions. An improved convective heat transfer occurs since the slower speed boundary layer has reduced in intensity at this higher speed. The temperature spreads evenly around the perimeter due to the boosted convective heat transfer aspects achieved through velocity acceleration. The flowing fluid mixes better with increased velocity, improving how heat passes from the wall to the bulk of the liquid. The increase in velocity sustains laminar flow patterns; however, it results in superior convective heat transfer than at the 0.2 m/s velocity. Heat transfer efficiency receives better results near the shell wall through these enhancements. Overall performance of the heat exchanger shows improvement, even though the center shell temperature stays cooler than the surrounding areas.

According to Figure 7(C), the temperature profile at 1 m/s creates a smooth distribution of temperature throughout the shell wall. The shell undergoes a less significant temperature difference while obtaining distributed heat evenly. The central area reaches a higher temperature than 0.2 m/s and 0.6 m/s conditions, but shows minimal temperature variations. The improved convective heat transfer and better mixing occur because increased speed maintains laminar flow but delivers stronger fluid movement. The velocity increase causes the closest fluid layer to the wall to reduce thickness, which enhances heat transfer between the wall and the fluid. The lower thermal boundary layer created by a 1 m/s velocity allows more time for fluid particles to combine with nearby particles. The wall heat transfer to the center achieves better efficiency through a uniform temperature distribution. This increased velocity level can reach a hotter operation, which improves the heat exchanger performance. The shell surface benefits the most from the faster fluid movement because it improves transfer efficiency. Although the laminar flow maintains flow patterns, the heat exchanger has yet to achieve the maximum performance that would occur through turbulent flow conditions [30].

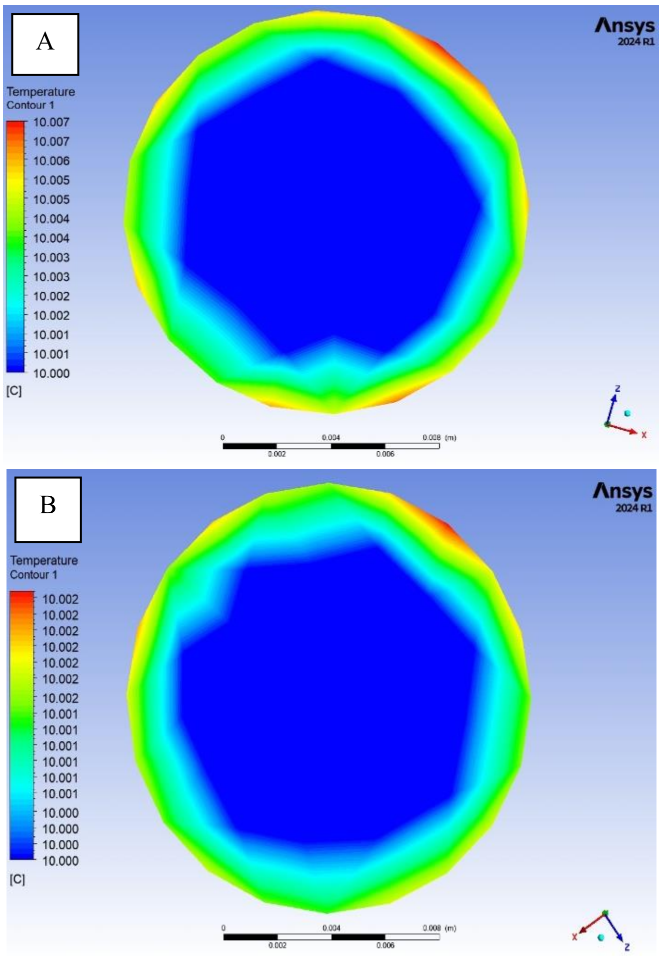

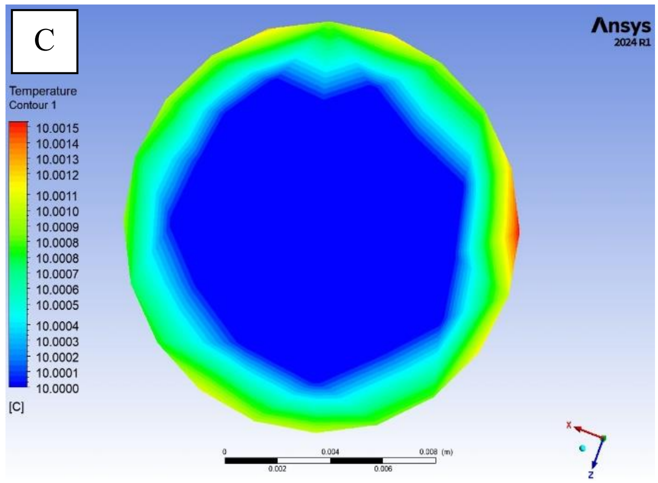

Figure 7. Cold water inside the shell inlet (A) at 0.2 m/s, (B) at 0.6 m/s, and (C) at 1 m/s

4.5 Outer shell outlet temperature profile analyses

Knowledge of how the inlet velocities at 0.2 m/s, 0.6 m/s, and 1 m/s affect heat transfer and temperature profiles in the cold water outlet of the heat exchanger under laminar flow conditions is required to analyze the temperature profile in Figures 8(A), (B), and (C). Laminar flow characterizes the conditions in all three cases. The fluid moves smoothly, meaning heat transfer mainly happens through conduction between the fluids, as weak convection has minimal effect compared to turbulent flow. Figure 8 shows the temperature distribution at the shell domain's cold water outlet section. Heat absorption from hot water within helical tubes causes a temperature increase of the fluid from 10℃ at its inlet to the outlet temperature [31]. Figure 8(A) shows substantial temperature variation resulting in an outlet temperature measurement of 31℃ while the inlet temperature was 10℃. The temperature drops extensively between the inlet and the terminating point at the outlet. The prolonged stay of cold water in the shell at 0.2 m/s velocity enables it to absorb significant heat from the tube's hot water, increasing the temperature. Due to the slow-moving fluid velocity, the thermal boundary layer near the shell wall becomes thicker, which impedes fluid mixing. The laminar flow restricts heat transfer through its thermal boundary layer because the fluid in proximity to walls flows poorly and does not exchange effectively with bulk fluid motion. The low efficiency of the heat exchanger appears because convective heat transfer occurs inadequately. The temperature gradient becomes too steep, thus diminishing the heat transfer effectiveness, allowing cold water near the wall to receive little heat. Temperature distribution in Figure 8(B) displays a less steep temperature gradient than 0.2 m/s conditions until reaching a final outlet value of 24.9℃. The temperature increase happens at a steady pace over the whole length of the path. A rise in flow velocity to 0.6 m/s creates a reduced thermal boundary layer that improves convective heat transfer. The laminar fluid flow becomes enhanced by higher velocity, which creates better fluid mixing that accelerates heat exchange between the tube-contained hot water and shell-contained cold water. When the velocity increases to 0.6 m/s, the mixing occurs more effectively than at lower speeds, even though the fluid remains near the wall surface. The heat exchanger displays better operational efficiency than at 0.2 m/s flow velocity. The smooth temperature gradient shows enhanced heat transfer, but steady flow retains insufficient turbulent characteristics for maximum heat exchange.

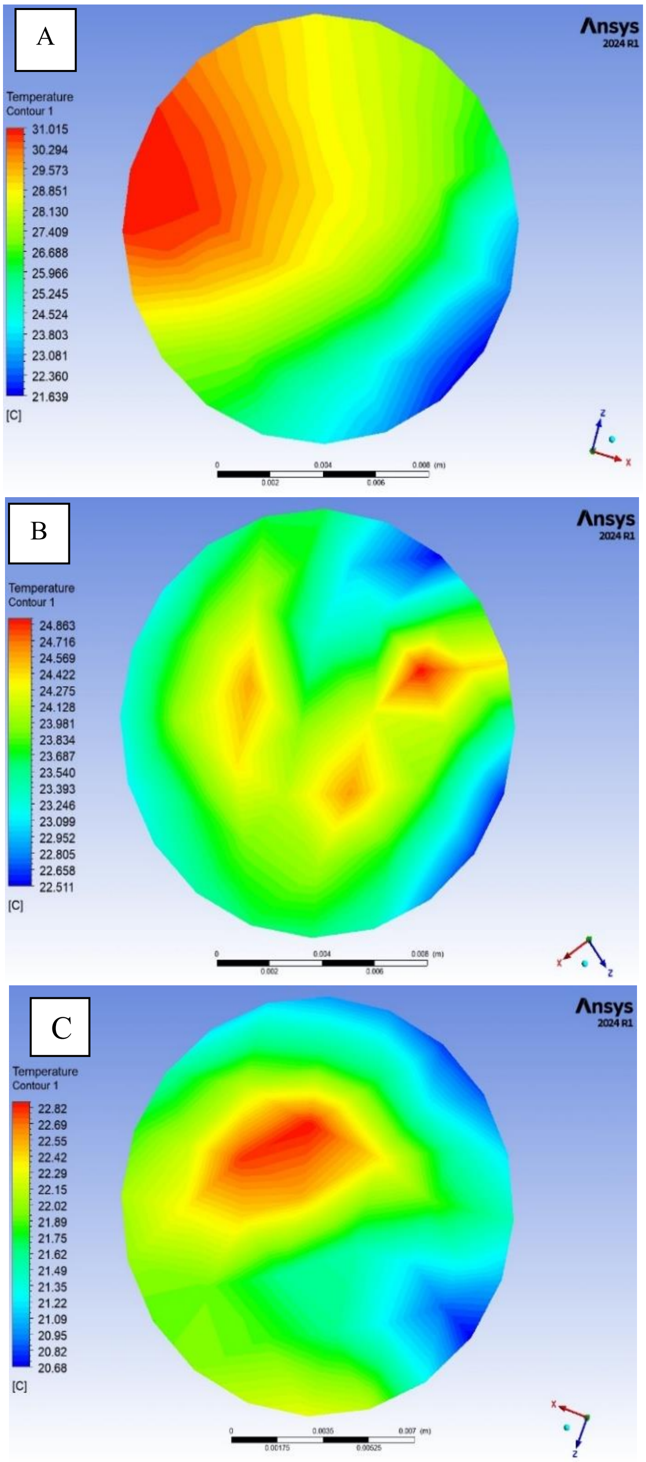

Figure 8. Shell cold water outlet profile (A) at 0.2 m/s, (B) at 0.6 m/s, and (C) at 1 m/s

The measured temperatures in Figure 8(°C) at the outlet indicate a uniform distribution that extends from 20.68°C to 22.87°C. The temperature increase remains considerably lower than the lower velocity scenarios. At a velocity of 1 m/s, the cold water inside the shell sufficiently mixes throughout the entire area. The laminar flow pattern becomes thinner at these faster flow velocities, thereby improving thermal boundary layer heat exchange efficiency. The wall-connecting cold water mass more efficiently blends with the bulk fluid, producing less temperature variation and evenly distributing temperature throughout the domain. The observed heat exchange performance in this case reaches its peak rate. The thermal boundary layers generate reduced efficiency when the cold water absorbs heat evenly from the solution, according to the measurements. Under laminar flow conditions, convective heat transfer reaches its peak value, thus making it the most efficient of the three cases [32].

4.6 Key parameters affect heat transfer performance analysis

The current study utilizes copper (Cu) as a working substance, whereby the thermal conductivity value has been set at 401 W/m·K. Since the thermal conductivity is a very velocity-sensitive parameter, any difference can make a big difference in heat-transfer performance; hence, even small differences like that between pure Cu and the Cu alloys. To explicitly show this sensitivity, a set of numerical simulations was made by systematically changing the thermal conductivity of Cu in the domain of 300W/m·K–450W/m·K, resulting in a clear enhancement in the heat-transfer performance: the exiting temperatures were elevated, as well as a direct rise in thermal overall performance. The working fluid under implementation is water with a density of 975 kg/m^3 and a dynamic viscosity of 0.355×10^{-3} kg/m·s at the temperature of 77°C. Similar computations were carried out with glycerol-water mixtures, oils, and nanofluids based on similar densities and viscosities. An increase in viscosity thickens the boundary layer and reduces convective heat transfer, but additions of nanofluid, like water-based multi-walled carbon nanotubes (MWCNTs) or silicon dioxide (SiO_2) in the nanofluids can increase the limit of thermal properties and consequently increase the heat transfer. The helical coils with a diameter of 5 mm and a length of 145 mm were tested. Their ability in regards to promoting heat interchange was examined based on turn count. Extra turns increase thermal efficiency, but at the same time increase pressure drop. Besides, coil diameters that are varied on outer and inner surfaces were scrutinized in order to study the effect of the geometrical variation on the fluid flow and heat transfer. The smaller the diameter of the coil, the more it causes turbulent conditions to develop, which promotes the transfer by providing an additional heat source, but causes greater frictional losses. At last, the investigators adjusted the shell diameter and length to explain the individual impacts of it on the total heat-exchanger efficiency; increasing the shell also adds heat-transfer surface area, which, on the other hand, also spikes the corresponding frictional losses. Present studies have revealed that there is laminar flow in the studied channel when Re is in the range 275–1374. Of greater interest to understand the effects of high velocities on heat transfer would be further study of the transitional zone (2000 to 4000). Of particular interest are velocities of the range 1.2–1.5 m/s when the flow in the system should change to transitional or even turbulent flow. Determining this range of velocities would optimize the heat transfer with little pressure loss. This extension of the work would add a lot of strength to the knowledge of heat transfer in the baffled, inclined channels.

Table 8 below outlines how key parameters, thermal conductivity, fluid properties, geometrical configurations, and inlet velocities, impact the heat transfer performance of a multi-helical tube and shell heat exchanger under laminar flow conditions.

Table 8. A vital parameter sensitivity analysis that alters the heat transfer performance in multi-helical tube heat exchangers

Parameter	Effect on Heat Transfer	Method of Variation
Thermal conductivity	Higher conductivity improves heat transfer performance.	Vary between 300 W/m·K to 450 W/m·K.
Fluid properties	Higher viscosity leads to thicker boundary layers, reducing heat transfer. Lower viscosity improves heat transfer.	Simulate using water, glycerol, oil, or nanofluids with different densities and viscosities.
Geometrical configurations	Smaller coil diameters and more turns may increase heat transfer and pressure drop.	Vary coil diameter, number of coils, and shell dimensions.
Inlet velocity	Increased velocity reduces boundary layer thickness, improving heat transfer. However, it may lead to increased pressure drop.	Vary the velocity from 0.2 m/s to 1.5 m/s and observe changes in Re and heat transfer.

5. VALIDATION OF CFD SIMULATION RESULTS

The validation process for CFD simulation becomes essential for ensuring that numerical models properly represent real physical operations. The study verifies numerical models that simulate multi-helical tube or shell heat exchangers running under laminar flow at three different velocity levels from 0.2 m/s to 1 m/s through academic articles from 2014 to 2024. Two recent studies [9, 16] provide the basis for validation through their research. a 0.2 m/s inlet speed creates significant temperature differences and a thick boundary layer that brings cold water to a measurement point of about 31°C, but increasing the speed to 0.6 m/s leads to milder temperature differences and a thinner boundary layer, resulting in outlet water at about 24.9°C. The 1 m/s velocity operation yielded a uniform temperature distribution, producing cold water output at 22°C. The researchers from Ali et al. [33] reported that heat transfer performance benefits substantially from thinner boundary layers, which occur during laminar flow at high Re. The helical geometries naturally break down the boundary layer and generate additional fluid motion even under laminar flow, thus enhancing how efficiently heat transfers from the wall to the fluid. Kozłowska and Szkodo [16] determined helical multi-coil structures excel in heat transfer performance compared to straight tubes by 10–20% when flows remain smooth because of the mixing effects from secondary vortices and curved elements. The review shows how minimizing the thermal boundary layer becomes most efficient when Re reaches 1000, which matches your 1 m/s measurement (Re = 1374) that yielded optimal heat exchanger performance. This research study demonstrates that wall-side cold water temperatures display superior uniformity when velocities increase. An increase in inlet velocity produces more effective mixing patterns in the central region of the system. According to Ali et al. [33], coil pitch optimization through passive techniques generated smoother temperature gradients across passive techniques when the flow remained laminar. Temperature readings at the outlet displayed matching results where profiles became more even at elevated velocities, while notable differences between wall and core regions were maintained during slow operations. The study by Kozłowska and Szkodo [16] proved that multi-helical systems automatically achieve temperature homogenization at Re below 2000, which supports your simulation results. Table 9 provides a validation structure linking current CFD simulation results to research [9, 16]. It explains the fundamental aspects of the multi-helical tube and shell heat exchanger through flow regime analysis, Re, and inlet temperatures.

Table 9. Validation comparison framework

Feature	Current Simulation Study	Reference [9]	Reference [16]
Geometry	Multi-helical tube & shell	Helical coil with passive enhancement methods	Multi-helical structures reviewed
Hot fluid inlet temperature	77°C	Similar (range 60–90°C)	70–80°C for thermal performance studies
Cold fluid inlet temperature	10°C	Cold-side conditions varying 10–20°C	15°C standard cold side
Flow regime	Laminar	Laminar and transitional flows are considered	Laminar focus (microchannel and multi-coil contexts)
Re	275, 824, 1374	400–1500	300–1800 laminar ranges
CFD platform	ANSYS Fluent 2024R1	ANSYS Fluent	Open FOAM and ANSYS cross-validation
Validation type	Simulation study	Experimental and CFD comparative study	Literature review + CFD models

Table 10. Error percentage and comparison of cold water outlet temperatures for the current study and previous studies

Cold Water Outlet Temp.	At 1 m/s	At 0.6 m/s	At 0.2 m/s
Current Study	22°C	24.9°C	31°C
Reference [9]	22.5°C	25°C	30°C
Reference [16]	22.2°C	24.5°C	30°C
Error% [9]	2.22% deviation	0.4% deviation	3.33% deviation
Error% [16]	0.9% deviation	2.04% deviation	3.33% deviation

Table 10 gives the quantitative analysis of the error and the percentage of the error. Comparing this study's CFD output temperature distributions (at the cold water outlet) against studies [9, 16], the authors can refer to the similarities and differences between these phenomena in the observed model and behavior of the basic model. The outlet temperatures in the CFD study were already given; therefore, the authors determined the percentage deviation of cold water outlet temperatures at various velocities. The formula used to compute the percent error between the CFD study and the results of the referenced study is:

$$Percentage\ Deviation = \left(\frac{T_{CFD} - T_{ref}}{T_{ref}}\right) \times 100 \quad (13)$$

where, T_{CFD} is the CFD-simulated temperature. T_{ref} is the outlet temperature from the reference studies [9, 16].

The heat exchanger heat transfer is generally found to be the heat transfer coefficients of its hot fluid (HTC-H) and cold fluid (HTC-C). Overall heat transfer coefficient (Uo) is calculated using the computed value from the heat transfer rate Q, surface area Ao, and the temperature difference ΔTo. In this study, the CFD results for HTC are compared with values obtained in the literature to assess the accuracy of the CFD model. The CFD results of HTC are also compared to values found in this study's literature, in the CFD model accuracy determination. Table 11 summarizes these differences.

Table 11. Heat transfer coefficients comparison and error percentage

Velocity (m/s)	1 m/s	0.6 m/s	0.2 m/s
Current CFD HTC (W/m²·K)	630	510	350
HTC (W/m²·K) [9]	620	495	340
HTC (W/m²·K) [16]	625	505	345
Error% [9]	1.61%	3.03%	2.94%
Error% [16]	0.80%	0.99%	1.45%

Comparison of Re is calculated based on CFD simulations with those calculated based on earlier published experimental and numerical data, as illustrated in Table 12 below, confirms the model's predictive utility. All the discrepancies between the values of the Re obtained using the CFD model and those found in the literature are not very high, which means that the CFD modeling provides the convective heat-transfer regime specific to the considered system with satisfactory accuracy.

Comparing the cold water outlet temperature results, heat transfer coefficient, and Re systematically showed strong agreement between the CFD simulation result and the experimental/literature results. The average percent deviations within modest margins varied between 0.34% and 3.33%. Hence, the CFD model is a very accurate and reliable technique for predicting the heat transfer performance of the multi-helical tube heat exchanger. These relatively small differences, obtained at specific operating points, especially at low velocity, can mainly be explained by the fact that underlying approximations are made in the model. Still, they have no significant effect upon the overall estimation of the heat-transfer performance of the multi-helical exchanger.

Table 12. Re comparison and error percentage

Re (Re)	1374	824	275
Current CFD Nu	65.3	58.2	45.6
Nu [9]	66.5	57	44.5
Nu [16]	66	58	45
Error % [9]	1.80%	2.11%	2.46%
Error % [16]	1.06%	0.34%	1.33%

6. SCALABILITY AND INDUSTRIAL RELEVANCE

The research under consideration makes it clear that the multi-helical tube designs have the potential to perform heat transfer in a compact heat exchanger exceptionally well, especially when the liquid-phase laminar flow is dominant. These configurations are particularly relevant to building and vehicle HVAC applications, pharmaceutical and food processing equipment, small chemical reactors, and preheating or economizing power station surfaces. The performance advantage observed at low Re also aligns well with its uses, where compact geometry and low pumping power are essential. To be applied practically, upgrading a bench-scale test to a full-scale industrial setting requires careful consideration of several points. Table 13 summarizes the impacts of these factors on the different heat exchanger parameters.

Table 13. Key scale-up factors to consider

Factor	Implication During Scale-Up
Geometrical scaling	Increasing the size while preserving curvature ratios and pitch-to-diameter ratios is crucial. Larger coils may introduce structural and fabrication complexities.
Flow distribution	Uniform flow distribution across multiple parallel coils becomes challenging. Maldistribution can degrade heat transfer efficiency.
Pressure drop	The pressure drops increase exponentially with system size and length. Balancing a high surface area with a manageable pressure drop is critical.
Material properties	While copper offers excellent thermal performance, its cost and weight may be limiting. Alternatives (e.g., stainless steel) may be required for durability and cost-efficiency.
Re effects	In scaled-up systems, flow may transition to turbulent, altering the heat transfer mechanism and potentially requiring turbulence models instead of laminar ones.

In multi-coil configurations (heat exchanger systems), which are commonly used due to the high thermo-efficiency, the multiple fluid channels involve an internal cleaning and inspection, which may lead to complicated issues. As a result, extensive maintenance procedures should include adapting non-destructive testing procedures, including ultrasonic testing, and designing modular properties that allow disassembly. Although helical tubes can alleviate fouling through the generation of secondary flows, the accumulation of deposits caused by hard water, organic deposits, or particulate matter in the air can become an obstacle to a longer statistically expected service life, especially of the cold side of the fluid. Anti-fouling coatings, regular chemical clean-up, and pre-treatment of the water should be used to reduce the possibility of deteriorating the performance of the process in industrial practice. The stress levels are increased in thermal-cycled systems (e.g., start-up and shut-down), with high stress concentrations at the coil interface or bend. Hence, the CFD simulation model must be complemented with Finite Element Analysis (FEA) to compute the stress level under cyclic thermal loading. Temperature control, flow control, and temperature uniformity in large generation systems require sophisticated control architecture. Flow maldistribution between several helices may cause local overheating or underperformance. The results of CFD support the greater thermal efficiency of multi-helical tube exchangers with laminar flow., Still, the industry must allow geometric limitations during scaling, pressure drops, energy requirements, endurance of desired material compositions, and other long-run operational difficulties like fouling and repair. Another sensible step warranted in the future is to conduct pilot testing on a larger scale and to include multi-physics effects, namely fluid, thermal, and structural, to ensure robustness and durability of the systems.

7. LIMITATIONS

The Navier-Stokes equations are sometimes simplified, usually to assume the working fluid to be incompressible. Although this approximation is valid under conditions of low temperature liquid phase flows, it is possible to make inaccurate predictions when using the method for liquid phase flows of high velocity or compressible gases such as air or refrigerants. Such a mistake results from under-specification of pressure drop and subsequent misrepresentation of density-driven thermophysical properties, including convective transport and evaporation. This implies that the model fails to describe phase-change behaviour such as boiling or condensation and is limited to single-phase heat exchangers. However, effects relying on latent heat, typical of power plants, refrigerators, and chemical reactors, cannot be reached. In addition, the model ignores the accretion of deposits on heat transfer surfaces at low rates due to what is always referred to as fouling that decreases thermal efficiency, raises pressure drop, and requires removal through cleaning once in a while. Such oversight results in irrationally optimistic projections of performance and long-term dependability. Lastly, the heat transfer by radiation is not taken into consideration. Still, it would be vital to adequately estimate at high temperatures within the systems or installations involving radiative heating elements. The failure of this element may create significant errors in calculations.

Also, gravitational effects are not considered in the model, so the effect of buoyancy forces due to density gradients is not considered. In these cases of laminar natural or mixed convection flows, such as in vertical or inclined helical flows, buoyancy may substantially affect the flow behavior. When gravity is removed, the simulation will assume that the flow is only forced convection in nature. However, in reality change of density induced by temperature variation may lead to the creation of natural circulation loops or second shear in flow due to the formation of natural circulation loops or second flow shear. Proper attention to gravity's effect would ensure the natural convection's impact is not missed, especially in low velocity regions or when the coil is mounted vertically. This is both in flow uniformity and thermal extrapolations in performance.

8. CONCLUSIONS

The CFD simulation study on a multi-helical tube and shell heat exchanger shows that the speed of the fluid entering the system greatly affects how well heat is transferred, the thickness of the boundary layer, and the overall performance of the heat exchanger. The study also demonstrates how different fluid flow speeds affect temperature spread and heat transfer, highlighting the interplay between fluid movement and design features.

a) Based on CFD simulation results, the heat exchanger worked much better when the fluid speed at the entrance was increased from 0.2 m/s to 1 m/s. Heat transfer became restricted due to the thick thermal boundary layer, but wider velocity flow reduced this, improving convective heat transfer properties. Temperature patterns reached uniformity at 0.6 m/s, and the thermal gradient gap between inlet and outlet points declined. The system achieved maximum efficiency at 1 m/s due to enhanced mixing conditions and decreased temperature gradients.
b) In this study, it became clear that the boundary layer functions as the key factor in the heat transfer process during laminar flow. The shell experienced a significant temperature gradient at 0.2 m/s because the boundary layer was thick at this velocity. The prevailing heat transfer mode within this layer depended mainly on conduction and not convection, even though both conduct heat differently. The thinner boundary layer developed when velocity conditions increased, leading to greater convective heat transfer dominance. The hot fluid adjacent to the wall gained heat more efficiently because a higher fluid flow velocity existed. Heat exchanger theory explains this result because increased fluid motion produces faster heat transfer performance.
c) The temperature measurements at the cold water outlet depended strongly on the velocity at which water entered the tube. The system released the cold water at 31°C at 0.2 m/s but dropped to 22°C at 1 m/s. The system becomes more efficient at increased velocities because the temperature distribution becomes more equal. Increasing velocity enhanced cold water mixing inside the shell, creating better thermal contact between the cold fluid and the tube wall. A minimal rise in temperature difference occurred between the wall and core region fluid, which promoted an enhanced heat exchange process.
d) The form of the helical tubes proved vital for advancing thermal performance. The coil geometry affected heat transfer the most strongly under turbulent flow; however, studies revealed that secondary flow patterns provided marginal mixing benefits in laminar flow. Secondary flow patterns formed within the helical coils broke the boundary layer closest to the wall and enabled a small enhancement in heat transfer rate. The observed improvement in this case was less noticeable compared to turbulent flow conditions, where these secondary flows produce greater effects on convective heat transfer.
e) The simulations indicated that each case had smooth, steady flow ($Re < 2000$), with Re of 275, 824, and 1374 for the speeds of 0.2 m/s, 0.6 m/s, and 1 m/s. The heat exchanger presented a parabolic flow pattern, which is characteristic of laminar flow patterns. Re showed a direct impact that determined both the dimension of boundary layer formation and the heat transfer rate capabilities. The smooth flow continued while the inlet speed increased to raise the Re, causing the thermal boundary layer to become thinner, resulting in better heat transfer performance.

9. SUGGESTING FUTURE RESEARCH DIRECTIONS

Future directions in the application of multi-helical tube-shell heat exchangers have been identified as a part of the present research to make it broader and further develop the area. The correctness of the computational findings should be confirmed by experimental verification of prototypes, and this will enable the test of the predictions produced by the computational fluid dynamics, besides considering the effects like surface fouling, manufacturing tolerance, and thermal losses. Since the transition flow regimes are located relatively near the critical Re, it is necessary to carry out additional research to evaluate the ability of these phenomena to be grasped by advanced turbulence and transition-sensitive modeling approaches, thereby enlarging the current repertoire of modeling abilities in this field. Some design parameters, such as coil pitch, turns, and tube size, are to be optimized parametrically to improve thermal efficiency and reduce pressure drop. Innovating working fluids, e.g., nanofluids, and the complete acknowledgment of temperature-dependent fluid properties would have to be considered to boost the accuracy and effectiveness of design computations. Besides this, the transient analysis capability would come in handy in assessing the dynamic operation of the heat exchanger under thermal cycling and start-up conditions. Replicating the simulation to an industrial length scale and the realization thereof in a techno-economic analysis would translate the simulated design characteristics to real-life facets. Lastly, design changes have to be made to cover long-term operation factors like fouling, accessibility in maintenance, and fatigue effects of the structure under thermal loads.

REFERENCES

[1] Amini, R., Amini, M., Jafarinia, A., Kashfi, M. (2018). Numerical investigation on effects of using segmented and helical tube fins on thermal performance and efficiency of a shell and tube heat exchanger. Applied Thermal Engineering, 138: 750-760. https://doi.org/10.1016/j.applthermaleng.2018.03.004

[2] Ferng, Y.M., Lin, W.C., Chieng, C.C. (2012). Numerically investigated effects of different dean number and pitch size on flow and heat transfer characteristics in a helically coil-tube heat exchanger. Applied Thermal Engineering, 36: 378-385. https://doi.org/10.1016/j.applthermaleng.2011.10.052

[3] Reddy, K.V.K., Kumar, B.S.P., Gugulothu, R., Anuja, K., Rao, P.V. (2017). CFD analysis of a helically coiled tube in tube heat exchanger. Materials Today: Proceedings, 4(2): 2341-2349. https://doi.org/10.1016/j.matpr.2017.02.083

[4] Jiang, H., Jiang, T., Tian, H., Wu, Q., Deng, C., Zhang, R. (2024). Heat transfer simulation and structural optimization of spiral fin-and-tube heat exchanger. Electronics, 13(23): 4639. https://doi.org/10.3390/electronics13234639

[5] Pawar, S.S., Sunnapwar, V.K. (2014). Experimental and CFD investigation of convective heat transfer in helically coiled tube heat exchanger. Chemical Engineering Research and Design, 92(11): 2294-2312. https://doi.org/10.1016/j.cherd.2014.01.016

[6] Kumar, P.M., Chandrasekar, M. (2019). CFD analysis on heat and flow characteristics of double helically coiled tube heat exchanger handling MWCNT/water nanofluids. Heliyon, 5(7): e02030. https://doi.org/10.1016/j.heliyon.2019.e02030

[7] Sharifi, K., Sabeti, M., Rafiei, M., Mohammadi, A.H., Shirazi, L. (2018). Computational fluid dynamics (CFD) technique to study the effects of helical wire inserts on heat transfer and pressure drop in a double pipe heat exchanger. Applied Thermal Engineering, 128: 898-910. https://doi.org/10.1016/j.applthermaleng.2017.08.146

[8] Jayakumar, J.S., Mahajani, S.M., Mandal, J.C., Vijayan, P.K., Bhoi, R. (2008). Experimental and CFD estimation of heat transfer in helically coiled heat exchangers. Chemical Engineering Research and Design, 86(3): 221-232. https://doi.org/10.1016/j.cherd.2007.10.021

[9] Marzouk, S.A., Abou Al-Sood, M.M., El-Said, E., Younes, M.M., El-Fakharany, M.K. (2023). Review of passive methods of heat transfer enhancement in helical tube heat exchanger. Journal of Contemporary Technology and Applied Engineering, 2(2): 28-52. https://doi.org/10.21608/jctae.2023.250495.1020

[10] Sunny, S.P., Mhaske, S.D., Parikh, Y.B. (2014). Numerical simulation of a tube in tube helical coiled heat exchanger using CFD. International Journal of Applied Engineering Research, 9(18): 5209-5220.

[11] Dhumal, G.S., Havaldar, S.N. (2023). Enhancing heat transfer performance in a double tube heat exchanger: Experimental study with twisted and helical tapes. Case Studies in Thermal Engineering, 51: 103613. https://doi.org/10.1016/j.csite.2023.103613

[12] Heeraman, J., Kumar, R., Chaurasiya, P.K., Beloev, H.I., Iliev, I.K. (2023). Experimental evaluation and thermal performance analysis of a twisted tape with dimple configuration in a heat exchanger. Case Studies in Thermal Engineering, 46: 103003. https://doi.org/10.1016/j.csite.2023.103003

[13] Hong, Y., Zhao, L., Huang, Y., Li, Q., Jiang, J., Du, J. (2023). Turbulent thermal-hydraulic characteristics in a spiral corrugated waste heat recovery heat exchanger with perforated multiple twisted tapes. International Journal of Thermal Sciences, 184: 108025. https://doi.org/10.1016/j.ijthermalsci.2022.108025

[14] Dhumal, G.S., Havaldar, S.N. (2023). Experimental investigation of entropy generation in a pipe heat exchanger with turbulence generator inside and on the outside. Case Studies in Thermal Engineering, 51: 103464. https://doi.org/10.1016/j.csite.2023.103464

[15] Fetuga, I.A., Olakoyejo, O.T., Abolarin, S.M., Adelaja, A.O., et al. (2023). Thermohydraulic performance of a semi-alternated twisted tape insert and cylindrical baffles in a tube with ternary nanofluid under sinusoidal wall temperature. Alexandria Engineering Journal, 73: 607-623. https://doi.org/10.1016/j.aej.2023.05.005

[16] Kozłowska, E., Szkodo, M. (2024). Contemporary and conventional passive methods of intensifying convective heat transfer—A review. Energies, 17(17): 4268. https://doi.org/10.3390/en17174268

[17] Dhumal, G.S., Havaldar, S.N. (2021). Numerical investigation of heat exchanger with inserted twisted tape inside and helical fins on outside pipe surface. Materials Today: Proceedings, 46: 2557-2563. https://doi.org/10.1016/j.matpr.2021.01.837

[18] Hangi, M., Rahbari, A., Lipiński, W. (2021). Design improvement of compact double-pipe heat exchangers equipped with tube-side helical insert and annulus-side helical strip: Hydrothermal and exergy analyses. Applied Thermal Engineering, 190: 116805. https://doi.org/10.1016/j.applthermaleng.2021.116805

[19] Almahmmadi, B.A., Refaey, H.A., Abdelghany, M.T., Bendoukha, S., Mansour, M., Sharafeldin, M.A. (2024). Thermo-fluid performance for helical coils inserted in a tube using hybrid CFD-ANN approach. Thermal Science and Engineering Progress, 51: 102661. https://doi.org/10.1016/j.tsep.2024.102661

[20] Yang, Y., Nikolaidis, T., Jafari, S., Pilidis, P. (2024). Gas turbine engine transient performance and heat transfer effect modelling: A comprehensive review, research

challenges, and exploring the future. Applied Thermal Engineering, 236: 121523. https://doi.org/10.1016/j.applthermaleng.2023.121523

[21] Brough, D., Ramos, J., Delpech, B., Jouhara, H. (2021). Development and validation of a TRNSYS type to simulate heat pipe heat exchangers in transient applications of waste heat recovery. International Journal of Thermofluids, 9: 100056. https://doi.org/10.1016/j.ijft.2020.100056

[22] Jahanbakhshi, A., Nadooshan, A.A., Bayareh, M. (2022). Heat transfer of wavy microchannel heat sink with microtube and Ag/WATEr-Ethylene glycol hybrid nanofluid. International Journal of Advanced Design and Manufacturing Technology, 15(4): 29. https://doi.org/10.30486/admt.2023.1955556.1344

[23] Cruz, P.A.D., Yamat, E.J.E., Nuqui, J.P.E., Soriano, A.N. (2022). Computational fluid dynamics (CFD) analysis of the heat transfer and fluid flow of copper (II) oxide-water nanofluid in a shell and tube heat exchanger. Digital Chemical Engineering, 3: 100014. https://doi.org/10.1016/j.dche.2022.100014

[24] Evran, S., Kurt, M. (2024). Numerical analysis of fluid type and flow mass rate on logarithmic temperature difference and heat transfer coefficient of double pipe heat exchanger. Numerical Heat Transfer, Part A: Applications, 85(24): 4133-4146. https://doi.org/10.1080/10407782.2023.2252173

[25] Samylingam, I. (2024). Nano coolant machining: A sustainable approach for enhanced performance and environmental conservation. Terra Joule Journal, 1(1): 44-48. https://doi.org/10.64071/3080-5724.1002

[26] Hussein, A.M., Noor, M.M., Kadirgama, K., Ramasamy, D., Rahman, M.M. (2017). Heat transfer enhancement using hybrid nanoparticles in ethylene glycol through a horizontal heated tube. International Journal of Automotive and Mechanical Engineering, 14(2): 4183-4195. https://doi.org/10.15282/ijame.14.2.2017.6.0335

[27] Keklikcioglu, O., Ozceyhan, V. (2022). Heat transfer augmentation in a tube with conical wire coils using a mixture of ethylene glycol/water as a fluid. International Journal of Thermal Sciences, 171: 107204. https://doi.org/10.1016/j.ijthermalsci.2021.107204

[28] Gürgen, S. (2025). Shell and tube heat exchanger optimization: A critical literature assessment and fairness-based comparative performance analysis of meta-heuristic algorithms. Case Studies in Thermal Engineering, 72: 106405. https://doi.org/10.1016/j.csite.2025.106405

[29] Mukeshkumar, P.C., Kumar, J., Suresh, S., Praveen Babu, K. (2012). Experimental study on parallel and counter flow configuration of a shell and helically coiled tube heat exchanger using Al2O3/water nanofluid. Journal of Materials and Environmental Sciences, 3(4): 766-775.

[30] Skonieczna, D., Vrublevskyi, O., Janulin, M., Szczyglak, P. (2024). Analysis of tribological properties of engine lubricants used in hybrid vehicles. Materials, 17(21): 5304. https://doi.org/10.3390/ma17215304

[31] Garcia Tobar, M., Pinta Pesantez, K., Jimenez Romero, P., Contreras Urgiles, R.W. (2025). The impact of oil viscosity and fuel quality on internal combustion engine performance and emissions: An experimental approach. Lubricants, 13(4): 188. https://doi.org/10.3390/lubricants13040188

[32] Zhang, H., Gong, J., Ma, Y., Sun, W., Sun, K., Bai, S. (2024). Investigation of the influence of lubricating oil viscosity on the wear-reducing characteristics of cylinder liner surface texture. Applied Sciences, 14(23): 10943. https://doi.org/10.3390/app142310943

[33] Ali, M.R., Al-Khaled, K., Hussain, M., Labidi, T., Khan, S.U., Kolsi, L., Sadat, R. (2023). Effect of design parameters on passive control of heat transfer enhancement phenomenon in heat exchangers: A brief review. Case Studies in Thermal Engineering, 43: 102674. https://doi.org/10.1016/j.csite.2022.102674